Complexation of planar, organic, five-membered cations with crown ethers

Sari Kiviniemi,[a] **Maija Nissinen,**[b] **Markku T. Lämsä,**[a] **Jorma Jalonen,**[a] **Kari Rissanen**[b] **and Jouni Pursiainen***[a]

[a] *Department of Chemistry, University of Oulu, PO Box 3000, Oulu, FIN-90401, Finland*
[b] *Department of Chemistry, University of Jyväskylä, PO Box 35, Jyväskylä, FIN-40351, Finland*
    E-mail: Jouni.Pursiainen@oulu.fi

Complexation of six aromatic, nitrogen-containing cations with various crown ethers has been studied using ^{1}H NMR, mass spectrometric and crystallographic methods. Hydrogen bonding appears to be the most important interaction in complexation, but minor effects such as π-stacking or cation–π interactions have also been observed. The stability constants of five different imidazolium perchlorate·crown ether complexes and five other similar cation·DB18C6 complexes were determined by ^{1}H NMR titration in acetonitrile solution. The stability of these complexes in solution and in the gas phase is discussed. The crystal structures of seven complexes were determined in order to study complexation in the solid state. Four of these are imidazolium complexes with different crown ethers and three are complexes of dibenzo-18-crown-6 with similar planar cations.

Introduction

Complexation of organic molecules *via* weak non-covalent interactions such as hydrogen bonding, π-stacking, charge-transfer interaction and electrostatic interactions is of great importance.[1] Of these interactions, cation–π, π-stacking and charge transfer have received increasing attention recently.[2] Cation–π and charge transfer interactions play an important role in various template, recognition and complexation phenomena in supramolecular chemistry.[3] In the crystalline state π-stacking readily occurs when planar aromatic moieties interact with each other, thus affecting the packing of the molecules.

From this point of view it is of particular interest that biologically important heterocyclic bases, like imidazole, form planar cations. As an effective structural unit at the active sites of various enzymes and nucleic acids imidazole has a key role in the biological function of these enzymes and nucleic acids. In its non-protonated form imidazole easily co-ordinates to transition metal ions like Zn^{2+} and can also form rather strong H-bonds. However, during enzymatic reactions imidazole can also exist as a protonated cation, and may then interact with the substrate by direct electrostatic or π–π-interactions.

It is already known that the imidazolium cation can form inclusion complexes with large crown ether-type hosts *via* H-bonding.[4,5] A stability constant (K) has been reported only for the complex of the 1,2,10,11,19,20-hexacarboxylate-27-crown-9 derivative with the imidazolium cation (350 M^{-1}).[5] The neutral imidazole molecule also forms complexes with some calixarenes and acridine derivatives; the stability constant for the complex of a calixarene type host and imidazole is 14 M^{-1} and for Rebek's diacid receptor and imidazole is 1.0×10^6 M^{-1}.[6,7]

In this work, we report the complexation of the imidazolium cation **1** with crown ethers with varying numbers of aromatic units. In addition, we have studied the complexation of 1-methyl- (**2**) and 1-phenylimidazolium (**3**), pyrazolium (**4**), 1,2,4-triazolium (**5**) and 1,3-thiazolium (**6**) cations with DB18C6 (dibenzo-18-crown-6). The complexes were charac-

terised by ^{1}H NMR, MS (FAB, ESI) and elemental analysis. We also report seven crystal structures of crown ether complexes; four imidazolium complexes with different crown ethers and three complexes of DB18C6 with pyrazolium, 1,2,4-triazolium and 1,3-thiazolium cations (Fig. 1). The crystal structures of the imidazolium and pyrazolium complexes with DB18C6 have been discussed in the preliminary report of this work.[8]

Results and discussion

Complexation in solution

All crown ethers studied formed 1 : 1 complexes with the cations **1–6** in organic solvents. The stability constants (K) for 1 : 1 complexation were measured in CD_3CN solution by NMR titration and are presented in Table 1. The differences in chemical shifts of free and complexed imidazolium and other cations are a linear function of host concentration (1/[host]), which indicates 1 : 1 stoichiometry.[9] Additionally, 1 : 1 complexation was observed by mass spectrometric (FAB, ESI) measurements. Surprisingly, one exception from this 1 : 1 stoichiometry, 18C6·2(**1**) (**9**), was observed in solid-state studies.

Complexation is mainly caused by H-bonding but either π-stacking or charge-transfer interactions also seem to have a minor contribution towards complexation. The solvent effect of these experiments is difficult to estimate and has not been discussed.

Imidazolium perchlorate **1** easily forms DB18C6·**1** (**7**), B18C6·**1** (**8**), 18C6·**1** (**9**), DB21C7·**1** (**10**) and DB24C8·**1** (**11**) complexes. In solution, where the stability constants have been measured using an excess of the host, the stoichiometry of the host–guest complexes is 1 : 1. Of these constants, the highest (40 dm^3 mol^{-1}) was measured for 18C6·**1** (**9**) and the lowest for complex **11** (8 dm^3 mol^{-1}). In complex **9**, H-bonding to the ether oxygen atoms is obviously responsible for complexation. The stability constants for complexes **7** and **8** are clearly lower than the corresponding value of complex **9**. The aromatic rings of the crown ether decrease the electron
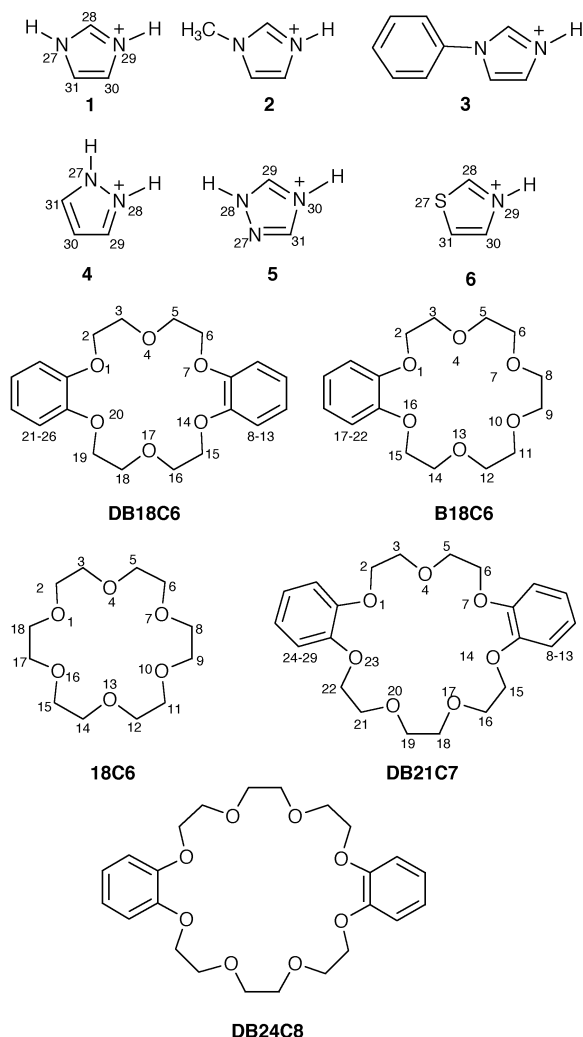
Fig. 1 Structural formulae of cations **1–6** and crown ethers showing the crystallographic numbering.

close to the corresponding value of the DB24C8·tropylium complex (10 dm³ mol⁻¹).[3d] This is surprising since the tropylium cation does not have a tendency for H-bonding. The crystal structure of the DB24C8·tropylium complex is a sandwich-like structure, in which the tropylium cation is π-stacked between the two benzene rings of the host.[3d] Assuming that complex **11** has a similar structure, the H-bonding between the host and the guest would not be sterically favoured since the ether oxygen atoms are not exactly in the same plane as the aromatic cation. It is known that the electron donor interactions between the tropylium cation and various benzene, naphthalene and anthracene donors in acetonitrile give stability constants of $K < 1$ M⁻¹ for the 1 : 1 complexes.[10] This seems to agree with the measured stability constant of the sandwich complex DB24C8·tropylium[3d] and, similarly, with complex **11**, where the oxygen atoms and the structure of the crown ether contribute to the stability. The crystal structure of the DB21C7·**1** complex, however, shows only hydrogen bonding and no π-stacking. Unfortunately, attempts to obtain single crystals of the DB24C8·**1** complex failed.

The stability constants of the 1-substituted methyl- (**2**) and phenylimidazolium (**3**) cations with DB18C6 (complexes **12** and **13**, respectively) are nearly 50% lower than the stability constant of the unsubstituted imidazolium complex **7** (Table 1). The stability constants of complexes **12** and **13** are almost equal indicating that the chemical nature and/or size of the substituent does not have a large effect on the stability of the complexes. Unfortunately we did not succeed in obtaining suitable single crystals for X-ray studies of complexes **12** and **13**.

The stability constant of the pyrazolium complex DB18C6·**4** (**14**) is more than twice as large (65 dm³ mol⁻¹) as the value of the corresponding imidazolium complex **7**. This can be rationalised by the suitable stereochemistry of two intracomplex hydrogen bonds acting simultaneously.

Without further investigations it is difficult to estimate why the third nitrogen atom of the triazolium ring **5** seems to decrease the stability of complex DB18C6·**5** (**15**, 18 dm³ mol⁻¹) compared to complex **7**, though complexes **15** and **7** have the same H-bonding possibilities. When compared to other complexes, it is interesting to note that the stability of complex **15** is closer to the stability of the 1-substituted complexes **12** and **13**.

The 1,3-thiazolium cation **6** has only one H-bond donating site. Owing to this fact, the stability constants of DB18C6·**6** (**16**, 32 dm³ mol⁻¹) and DB18C6·**1** (**7**, 27 dm³ mol⁻¹) are expected to be close to each other, indicating a similar H-bonding strength. This seems to indicate that the stereochemistry of the two N–H units on imidazolium does not favour formation of two H-bonds to the same crown ether, in contrast to the pyrazolium complex **14**.

density of the adjacent oxygen atoms, and this seems to decrease the strength of any H-bonding in complexes **7** and **8**, explaining the lower stability constants. In principle, complexes **7** and **8** have the potential for π-stacking and/or charge transfer interactions. Complex **7**, however, is much more stable (27 dm³ mol⁻¹) than the corresponding tropylium (C₇H₇⁺) complex ($K \approx 6$ dm³ mol⁻¹),[3d] indicating the dominant role of H-bonds in the former compound. The relative significance of different types of interaction is, however, difficult to estimate.

The stability constants of DB21C7·**1** (**10**, 10 dm³ mol⁻¹) and DB24C8·**1** (**11**, 8 dm³ mol⁻¹) are nearly equal and also

Table 1 The stability constants (K) of complexes between crown ethers and five-membered aromatic cations in CD₃CN solution at 30 °C determined by ¹H-NMR titration

Complex	K/dm³ mol⁻¹	$\Delta\delta_C{}^a$ (ppm)	$r^{2\,b}$
DB18C6·**1** (**7**)	27 ± 1	0.51 ± 0.01	0.999
B18C6·**1** (**8**)	25 ± 1	0.62 ± 0.01	0.999
18C6·**1** (**9**)	40 ± 1	0.563 ± 0.004	0.999
DB21C7·**1** (**10**)	10 ± 1	0.35 ± 0.04	0.997
DB24C8·**1** (**11**)	8 ± 1	0.36 ± 0.04	0.993
DB18C6·**2** (**12**)	18 ± 2	0.40 ± 0.03	0.998
DB18C6·**3** (**13**)	16 ± 2	0.51 ± 0.01	0.999
DB18C6·**4** (**14**)	65 ± 1	0.463 ± 0.004	0.999
DB18C6·**5** (**15**)	18 ± 2	0.48 ± 0.03	0.994
DB18C6·**6** (**16**)	32 ± 1	−0.46 ± 0.01	0.999

[a] Calculated maximum upfield/downfield shifts ($\Delta\delta_C$) for the interaction of crown ethers and aromatic cations in 1 : 1 complexation. [b] Regression correlation (r^2) for the Benesi–Hildebrandt plot.[11]

Complexation studies by mass spectrometric measurements

The complex formation was also studied by FAB-MS and ESI-MS (electrospray ionisation) measurements. FAB-MS-spectra showed 1 : 1 complexation in gas phase, since no sign of peaks with any other stoichiometry was observed (Table 2). The intensities of the corresponding peaks of the complexes were usually weak, under 5%, yet always detectable. The only exception is complex **9**, the intensity of the peak for the 1 : 1 complex of which was 12%. This supports the stronger stability of complex **9** compared to complexes **7**, **8** and **10** as also observed in solution. The base peak in the spectra was generally one heterocyclic cation under study. The FAB-MS results are in agreement with the solution and solid-state studies.

ESI mass spectra of complexes **7–15** confirm the FAB studies. Usually the only peak seen in the spectrum was at the complex ion mass, and sodiated crown ether or protonated crown ether was also occasionally present. In the ESI mass spectra of complexes **1** and **15** there was some indication of 2 : 1 complex formation where the protonated guest molecule formed a complex with two DB18C6 molecules in the gas phase.

X-Ray crystallography and solid-state complexes

The single crystal structures of the DB18C6 complexes **7**, **14**, **15** and **16** were determined; the 1-methyl- and 1-phenyl-imidazolium complexes **12** and **13** did not form suitable crystals for X-ray analysis. In addition the structures of B18C6·**1** (**8**), 18C6·**1** (**9**) and DB21C7·**1** (**10**) were determined for comparison with the DB18C6 complexes.

In the crystalline state all the DB18C6 complexes (**7**, **14–16**) show a very close resemblance. They all crystallise in an acentric monoclinic space group (*Cc*) with similar unit cells and nearly isomorphous structures. The complexes **8**, **9** and **10**, however, crystallise completely differently from the DB18C6 complexes and from each other. The complexes **8** and **9** crystallise out in centric monoclinic space groups ($P2_1/n$ and $P2_1/c$, respectively) while complex **10** crystallises in the orthorhombic, acentric space group ($P2_12_12_1$). However, all complexes pack into one-dimensional columns with perchlorate anions filling the intracolumnar space.

DB18C6 is a fairly rigid, bowl-like host with two possible sites for interactions with the guest: the minor site formed by the O–CH$_2$–CH$_2$–O chains and the major site located between the phenyl rings. The minor site may interact with the guest molecules only *via* hydrogen bonds while the major site can complex both *via* H-bonding and π-interactions. The inclusion of a guest capable of interacting with both sites (like the guests studied here) leads to interesting columnar packing in the crystalline state.

π-Stacking, however, plays only a minor role in the crystalline state interactions of DB18C6 complexes since the distances between the centroids of the cations and the closest phenyl ring are approximately 4.1 Å in all complexes. Hydrogen bonds, on the other hand, are relatively strong in all complexes; the interatomic distance of hydrogen-bonded

non-hydrogen atoms varies from 2.74 to 3.19 Å. The strongest H-bonding is observed in pyrazolium complex **14** where two intracomplex H-bonds N27···O17 [2.71(1) Å] and N28···O4 [2.788(9) Å] are formed.[8] The imidazolium and triazolium cations in complexes **7** and **15** are both hydrogen bonded to two adjacent hosts, but the bonding of the imidazolium cation is somewhat weaker than the bonding of triazolium. In both cases four hydrogen bonds are formed. In the case of triazolium the strongest hydrogen bond is N27···O17 [2.738(6) Å] and the weakest N20···O20 [3.112(6) Å] and the hydrogen bonds to an adjacent host are of intermediate strength [N30···O7* = 2.989(6) Å and N30···O14* = 2.956(6) Å]. The respective hydrogen bonds of the imidazolium cation are N27···O4 [2.824(7) Å], N27···O1 [3.193(7) Å] and to the adjacent host N29···O1* [3.023(7) Å] and N29···O20* [3.050(7) Å] (Fig. 2).

The most sterically crowded packing is observed with the thiazolium complex **16** since sulfur–carbon bonds are significantly longer than nitrogen–carbon and carbon–carbon bonds. Therefore the ring size of the thiazolium cation is also bigger than the size of the other cations investigated. The thiazolium cation has two different orientations in the complex due to the disorder between sulfur and carbon C31 with site occupancies of 0.561 and 0.439. In the more populated orientation C31 is pointing into the middle of the cavity of the host and the sulfur interacts with the ether oxygen atoms O14, O17 and O20 of the other edge of the cavity. In the less populated orientation the sulfur is buried deeply, exactly in the middle of the cavity, and it interacts with all of the ether oxygens (3.1–3.3 Å). The nitrogen of the thiazolium cation is hydrogen bonded to the adjacent host thus stabilising the column formation [N29···O7 = 2.895(5) Å and N29···O14 = 2.905(5) Å].

The inclusion of a guest, which interacts with both sites simultaneously during the packing, creates a one-dimensional
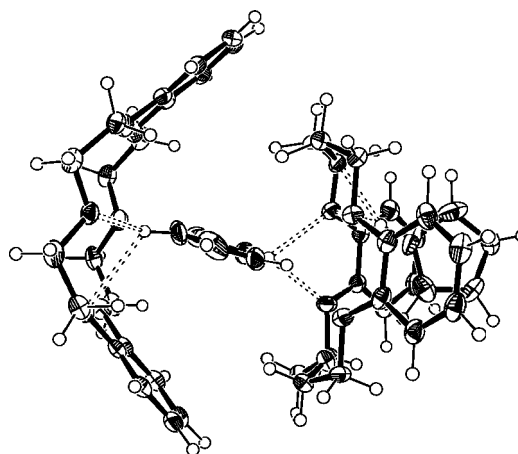

Fig. 2 ORTEP-3[12] plot of complex **7** (DB18C6·**1**). The imidazolium cation is hydrogen bonded (shown as broken bars) to two adjacent hosts. The perchlorate anions are excluded for clarity and the thermal ellipsoids are drawn at the 50% probability level.

Table 2 Selected peaks from positive ion FAB-MS-spectra of crown ether·cation complexes **7–10** and **12–15** (1 : 1 mixture) in NBA matrix

Crown ether	Ion (*m/z*) and relative abundance (%)
DB18C6·**1** (**7**)	69(100) C$_3$N$_2$H$_5$$^+$, 360(2.9) [DB18C6]$^+$, 429(3.2) [DB18C6·C$_3N_2H_5$]$^+$
B18C6·**1** (**8**)	69(100) C$_3$N$_2$H$_5$$^+$, 312(1.4) [B18C6]$^+$, 381(4.6) [DB18C6·C$_3N_2H_5$]$^+$
18C6·**1** (**9**)	69(100) C$_3$N$_2$H$_5$$^+$, 265(1.4) [18C6 + H]$^+$, 333(12.1) [18C6·C$_3N_2H_5$]$^+$
DB21C7·**1** (**10**)	69(100) C$_3$N$_2$H$_5$$^+$, 404(1.1) [DB21C7]$^+$, 473(2.8) [DB18C6·C$_3N_2H_5$]$^+$
DB18C6·**2** (**12**)	83(100) C$_4$N$_2$H$_7$$^+$, 360(1.8) [DB18C6]$^+$, 443(1.8) [DB18C6·C$_3N_2H_5$]$^+$
DB18C6·**3** (**13**)	145(100) C$_9$N$_2$H$_9$$^+$, 360(1.8) [DB18C6]$^+$, 505(1.8) [DB18C6·C$_3N_2H_5$]$^+$
DB18C6·**4** (**14**)	69(100) C$_3$N$_2$H$_5$$^+$, 360(2.9) [DB18C6]$^+$, 429(3.2) [DB18C6·C$_3N_2H_5$]$^+$
DB18C6·**5** (**15**)	55(100) [C$_2$N$_3$H$_4$ − NH]$^+$, 70(65) C$_2$N$_3$H$_4$$^+$, 360(2.9) [DB18C6]$^+$, 361(5.7) [DB18C6 + H]$^+$, 430(6.4) [DB18C6·C$_3N_2H_5$]$^+$

array of host–guest complexes with a 90° turn between the adjacent DB18C6 molecules and thus the small, planar guests are tightly encapsulated between the hosts (Fig. 2). Although formally all the DB18C6 complexes are 1 : 1 complexes both in solution and in the crystalline state, the crystal packing can only be described as 2 : 2 complexes. In the crystalline state, complexes **7** and **14–16** form one-dimensional arrays which all pack in the same direction, thus creating a polar axis into the crystal lattice. The polar axis of the crystal is caused by the weak interaction of the adjacent one-dimensional arrays. The perchlorate anions are located in between the columns, thus filling the voids in the crystal lattice.

The B18C6 is a more flexible and less symmetrical host than DB18C6, therefore such distinctive interaction sites cannot be identified. However, the simultaneous π–π and hydrogen bonding interactions between the host and the guest are still possible. In the crystalline state complex **8** did not show any π-stacking interactions (the closest distance between the centroids of the host and the guest is ≈4.7 Å), but a relatively strong hydrogen bonding pattern was observed. Complex **8** is also clearly a 2 : 2 complex in the crystalline state *i.e.* the host adopts two different conformations and two guest molecules themselves orient somewhat differently. The conformation of one host is bowl-like while the other could be described as almost planar (Fig. 3). The imidazolium located in the cavity of the bowl-like host is hydrogen-bonded to both hosts [N29A···O13A = 2.804(3) Å, N29A···O10A = 2.951 Å, N27A···O7B = 2.782(3) Å and N27A···O10B = 3.169(3) Å], while the other guest has only one relatively weak hydrogen bond to the planar-like host [N27B···O4B = 2.940(4) Å].

In contrast to the DB18C6 complexes, complex **8** packs into centrosymmetrical columns. The adjacent columns orienting in opposite directions show weak intermolecular π–π interactions (≈3.7 Å) between the edges of the phenyl rings. The 2 : 2 complexes are also readily distinguishable from the packing diagram since a larger space is left between the packages of two hosts and guests. Perchlorate anions again fill the voids between the columns.

Interestingly, 18C6 forms a 1 : 2 host–guest complex **9** with two imidazolium guests between each host (the asymmetric unit contains two guests and two halves of the host). The host–guest complex formation occurs *via* moderately strong hydrogen bonds [N27A···O1B = 2.746(3) Å, N29B···O4A = 2.861(3) Å and N29B···O1A = 3.100 Å]. In addition to host–guest hydrogen bonding there are hydrogen bonds between the cation and perchlorates [N27B···O105 = 2.893(3) Å and N29B···O102 = 2.856(3) Å] due to relatively open packing compared to deeply included DB18C6 and B18C6 in complexes **7** and **8**. The open packing is due to the orientation of the hosts and the guests between them (Fig. 4) leaving more space for interactions with inter-columnar anions. Also in this case the formation of a centrosymmetric column lattice is observed.
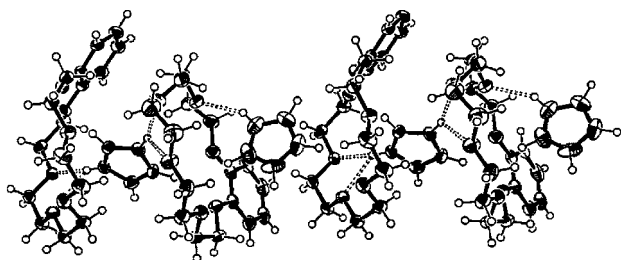

Fig. 4 The ORTEP-3[12] plot of complex **9** (18C6·**1**) which is exceptionally a 1 : 2 complex in the solid state. The hydrogen bonds are shown as broken bars and the thermal ellipsoids are drawn at the 50% probability level. The perchlorate anions are excluded for clarity.
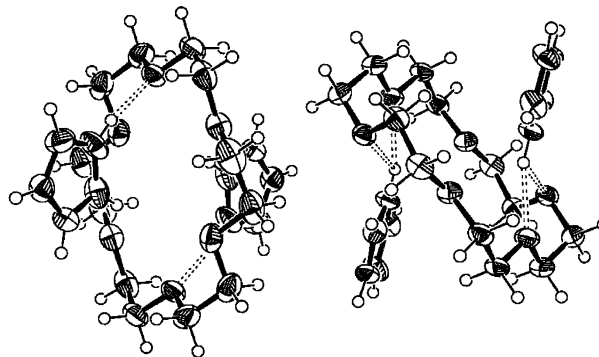
DB21C7, like DB18C6, is a bowl-like host with two possible interaction sites. However, the host also has more conformational flexibility and a bigger ring size than DB18C6 owing to the extra –CH$_2$–CH$_2$–O– chain. These features ensure that π-stacking has no role in the crystalline state complexation, leaving hydrogen bonds as the only interactions affecting complexation. However, the hydrogen bonding is also fairly weak: imidazolium shows only two, weak hydrogen bonds of equal length to ether oxygen atoms O23 and O1 [N30···O1 = 2.97(1) Å and N30···O1 = 2.99(1) Å]. Instead the imidazolium is more strongly hydrogen-bonded to the perchlorate anion [N32···O101 = 2.88(1)]. This is possible since the guest is not in the cavity of the host (Fig. 5) because of the interesting self-inclusion of the hosts: the longer crown ether chain forms a loop of a size suitable to fit the cavity of the adjacent host leaving no room for the guest inclusion. Thus the guests are hydrogen-bonded to the outside grooves of the chiral columns formed by the self-complementary hosts.

Conclusions

The stability of complexes between planar, five-membered cations and crown ethers was studied. Crown ethers containing aromatic units offer possibilities for weak interactions like hydrogen bonding through their crown oxygen atoms, and π–π-stacking or cation–π interactions through the electron-rich face of their aromatic rings. The complexes studied are stable enough and can easily be studied in the gas phase, in solution and in the solid state. We have found that the studied com-
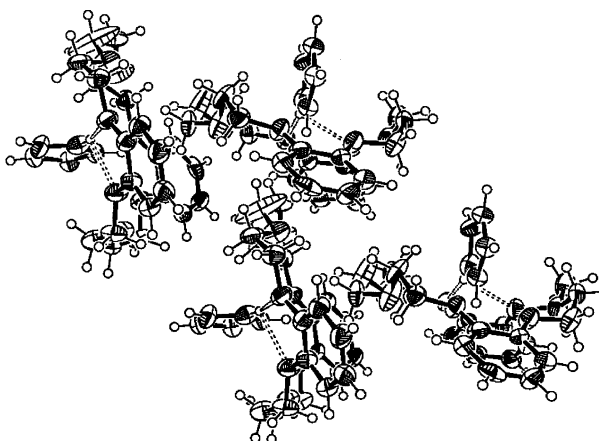

Fig. 3 A packing diagram of complex **8** (B18C6·**1**). The host adopts two different conformations: bowl-like and almost planar. The hydrogen bonds are shown as broken bars and the thermal ellipsoids are drawn at the 50% probability level. The perchlorate anions are excluded for clarity.

Fig. 5 A packing diagram of complex **10** (DB21C7·**1**). The hosts are self-included and thus the guests are hydrogen bonded (shown as broken bars) to outside grooves of the chiral columns formed by the hosts. The thermal ellipsoids are drawn at the 50% probability level and the perchlorate anions are excluded for clarity.

plexes are mainly stabilised by hydrogen bonds, and π–π-stacking or cation–π interactions play only a secondary role.

The X-ray studies reveal similar packing for all complexes in the solid state. All solid state complexes, except for 18C6·1 (9), are 1 : 1 complexes and thus agree with the solution and gas phase studies. 18C6·1, however, crystallised as a 1 : 2 complex probably due to the symmetrical nature of 18C6 and its ability to form simultaneous intracomplex H-bonds with two different protonated guests.

Experimental

General procedures

^{1}H NMR spectra were recorded on a Bruker AM200 spectrometer. EI and FAB mass spectra were obtained on a Kratos MS 80 mass spectrometer using the DART data system. ESI mass spectra were recorded on a LCT (Micromass Ltd) mass spectrometer with OpenLynx 3 data system. Elemental analysis was carried out with a Perkin-Elmer 2400. Melting points were determined with a Thermopan microscope (Reichert, Vienna). Imidazole, 1-methylimidazole, 1-phenylimidazole, pyrazole, 1,2,4-triazole, 1,3-thiazole, CD$_3$CN and all crown ethers were commercially available and used without further purification. Acetonitrile, dichloromethane, diethyl ether and other solvents were dried and distilled according to literature procedures.[13]

Preparation of perchlorates and complexes

The guest perchlorate salts were prepared according to literature procedures by treating the base with 60% perchloric acid.[14] The preparation of the complexes is straightforward. The cation perchlorates and crown ethers were dissolved in acetonitrile and the solutions were combined. The crystalline complexes either precipitated immediately from the reaction mixture or after addition of diethyl ether. The complexes were characterised by ^{1}H NMR-spectra, elemental analysis, FAB-MS and ESI-MS.

Imidazolium perchlorate 1. Yield 70%, mp 300 °C (decomp.). ^{1}H NMR (CD$_3$CN, 25 °C): δ 7.4 (d, 2H), 8.6 (s, 1H), 11.8 (t, NH, 2H). C$_3$H$_5$N$_2$ClO$_4$ (168.54): calcd C 21.38, H 2.99, N 16.62; found C 21.47, H 2.99, N 16.51%.

1-Methylimidazolium perchlorate 2. Yield 44%, mp 156–158 °C. ^{1}H NMR (CD$_3$CN, 25 °C): δ 3.9 (s, NCH$_3$, 3H), 7.4 (m, 2H), 8.5 (s, 1H), 11.6 (t, NH, 1H). C$_4$H$_7$N$_2$ClO$_4$ (182.56): calcd C 26.32, H 3.86, N 15.34; found C 26.45, H 3.64, N 15.29%.

1-Phenylimidazolium perchlorate 3. Yield 97%, mp 140–142 °C. ^{1}H NMR (CD$_3$CN, 25 °C): δ 7.6 (m, 6H), 7.8 (q, 1H), 8.9 (m, 1H), 12.1 (t, NH, 1H). C$_9$H$_9$N$_2$ClO$_4$ (244.63): calcd C 44.19, H 3.71, N 11.45; found C 42.90, H 3.29, N 10.91%.

Pyrazolium perchlorate 4. Yield 21%, mp 230 °C (decomp.). ^{1}H NMR (CD$_3$CN, 25 °C): δ 6.8 (t, 1H), 8.2 (d, 2H), 11.4 (s, NH, 2H). C$_3$H$_5$N$_2$ClO$_4$ (168.54): calcd C 21.38, H 2.99, N 16.62; found C 21.49, H 2.82, N 16.55%.

1,2,4-Triazolium perchlorate 5. Yield 42%, mp 225–228 °C. ^{1}H NMR (CD$_3$CN, 25 °C): δ 9.0 (s broad, 2H), 12.7 (t, NH, 2H). C$_2$H$_4$N$_3$ClO$_4$ (169.53): calcd C 14.17, H 2.38, N 24.79; found C 14.16, H 2.33, N 24.14%.

Thiazolium perchlorate 6. Yield 60%, mp 213–216 °C. ^{1}H NMR (CD$_3$CN, 25 °C): δ 8.1 (s, 1H), 8.2 (d, 1H), 9.8 (dd, 1H), 13.0 (s weak, NH, 1H). C$_3$H$_4$NSClO$_4$ (185.59): calcd C 19.42, H 2.17, N 7.55; found C 19.56, H 2.26, N 7.52%.

DB18C6-Imidazolium perchlorate 7. Yield 54%, mp 215–220 °C. ^{1}H NMR (CD$_3$CN, 25 °C): δ 3.8 (m, OCH$_2$, 8H), 4.1 (m, OCH$_2$, 8H), 6.9 (s, aryl, 8H), 7.4 (d, imidazolium, 2H), 8.8 (t, imidazolium, 1H). C$_{23}$H$_{29}$N$_2$ClO$_{10}$ (528.93): calcd C 52.23, H 5.53, N 5.30; found C 52.70, H 5.50, N 5.31%.

B18C6-Imidazolium perchlorate 8. Yield 55%, mp 124–126 °C. ^{1}H NMR (CD$_3$CN, 25 °C): δ 3.6 (s, OCH$_2$, 12H), 3.7 (m, OCH$_2$, 4H), 4.1 (m, OCH$_2$, 4H), 6.9 (s, aryl, 4H), 7.4 (d, imidazolium, 2H), 8.8 (t, imidazolium, 1H). C$_{19}$H$_{29}$N$_2$ClO$_{10}$ (480.90): calcd C 47.46, H 6.08, N 5.83; found C 47.38, H 6.08, N 5.77%.

18C6-2(Imidazolium perchlorate) 9. Yield 60%, mp 155–162 °C. ^{1}H NMR (CD$_3$CN, 25 °C): δ 3.5 (s, OCH$_2$, 24H), 7.4 (d, 2 × imidazolium, 4H), 8.7 (s, 2 × imidazolium, 2H). C$_{18}$H$_{34}$N$_4$Cl$_2$O$_{14}$ (601.39): calcd C 35.95, H 5.70, 9.32; found C 36.08, H 5.75, N 9.28%.

DB21C7-Imidazolium perchlorate 10. Yield 72%, mp 125–128 °C. ^{1}H NMR (CD$_3$CN, 25 °C): δ 3.7 (s, OCH$_2$, 4H), 3.8 (m, OCH$_2$, 4H), 3.9 (m, OCH$_2$, 4H), 4.1 (m, OCH$_2$, 8H), 6.9 (s, aryl, 8H), 7.4 (s, imidazolium, 2H), 8.6 (s, imidazolium, 1H). C$_{25}$H$_{33}$N$_2$ClO$_{11}$ (572.99): calcd C 52.40, H 5.80, N 4.89; found C 52.22, H 5.59, N 4.89%.

DB18C6-1-Methylimidazolium perchlorate 12. Yield 54%, mp 188–192 °C. ^{1}H NMR (CD$_3$CN, 25 °C): δ 3.8 (m, 1-Me-imidazolium NCH$_3$ and OCH$_2$, 12H), 4.1 (m, OCH$_2$, 8H), 6.9 (s, aryl, 8H), 7.3 (t, 1-Me-imidazolium, 1H), 7.4 (t, 1-Me-imidazolium, 1H), 8.6 (s, 1-Me-imidazolium, 1H). C$_{24}$H$_{31}$N$_2$ClO$_{10}$ (542.97): calcd C 53.09, H 5.75, N 5.16; found C 53.13, H 5.29, N 5.19%.

DB18C6-1-Phenylimidazolium perchlorate 13. Yield 69%, mp 147–151 °C (decomp.). ^{1}H NMR (CD$_3$CN, 25 °C): δ 3.9 (m, OCH$_2$, 8H), 4.1 (m, OCH$_2$, 8H), 6.9 (s, aryl, 8H), 7.6–7.5 (m, 1-Ph-imidazolium, 6H), 7.7 (t, 1-Ph-imdazolium, 1H), 9.0 (t, 1-Ph-imidazolium, 1H). C$_{29}$H$_{33}$N$_2$ClO$_{10}$ (605.03): calcd C 57.57, H 5.50, N 4.63; found C 57.69, H 5.25, N 4.63%.

DB18C6-Pyrazolium perchlorate 14. Yield 62%, mp 210–215 °C. ^{1}H NMR (CD$_3$CN, 25 °C): δ 3.9 (m, OCH$_2$, 8H), 4.1 (m, OCH$_2$, 8H), 6.6 (t, pyrazolium, 1H), 6.9 (s, aryl, 8H), 8.1 (d, pyrazolium, 2H). C$_{23}$H$_{29}$N$_2$ClO$_{10}$ (528.93): calcd C 52.23, H 5.53, N 5.30; found C 52.14, H 5.10, N 5.36%.

DB18C6-1,2,4-Triazolium perchlorate 15. Yield 32%, mp 187–189 °C. ^{1}H NMR (CD$_3$CN, 25 °C): δ 3.8 (m, OCH$_2$, 8H), 4.1 (m, OCH$_2$, 8H), 6.9 (s, aryl, 8H), 9.1 (s, 1,2,4-triazolium, 2H). C$_{22}$H$_{28}$N$_3$ClO$_{10}$ (529.93): calcd C 49.86, H 5.33, N 7.93; found C 50.04, H 4.91, N 7.87%.

DB18C6-Thiazolium perchlorate 16. Yield 86%, mp 209–213 °C. ^{1}H NMR (CD$_3$CN, 25 °C): δ 3.8 (m, OCH$_2$, 8H), 4.1 (m, OCH$_2$, 8H), 6.9 (s, aryl, 8H), 7.9 (dd, thiazolium, 1H), 8.2 (dd, thiazolium, 1H), 9.9 (m, thiazolium, 1H). C$_{23}$H$_{28}$NSClO$_{10}$ (545.99): calcd C 50.60, H 5.17, N 2.57; found C 50.60, H 5.01, N 2.69%.

Stability constant determination by ^{1}H NMR titration

A standard solution of guest in CD$_3$CN was prepared with a concentration of $(1–3) \times 10^{-3}$ M, just sufficient to give an observable NMR signal. A series of donor solutions (0.01–0.2 M) were made by weighing out an appropriate amount of donor. A 1–2 ml portion of the standard solution was then added and the flask was re-weighed. The solutions were mixed thoroughly and the spectrum was measured immediately. The temperature was held constant during the measurements. The

Table 3 Crystal data and data collection parameters

Complex	7	14	15	16	8	9	10
Formula	$C_{20}H_{24}O_6 \cdot$ $C_3H_5N_2^+ \cdot ClO_4^-$	$C_{20}H_{24}O_6 \cdot$ $C_3H_5N_2^+ \cdot ClO_4^-$	$C_{20}H_{24}O_6 \cdot$ $C_2H_4N_3^+ \cdot ClO_4^-$	$C_{20}H_{24}O_6 \cdot$ $C_3H_4NS^+ \cdot ClO_4^-$	$C_{16}H_{24}O_6 \cdot$ $C_3H_5N_2^+ \cdot ClO_4^-$	$C_{12}H_{24}O_6 \cdot$ $2C_3H_5N_2^+ \cdot 2ClO_4^-$	$C_{22}H_{28}O_7 \cdot$ $C_3H_5N_2^+ \cdot ClO_4^-$
M_r	528.93	528.93	529.93	545.99	480.90	601.39	572.99
a/Å	17.802(4)	17.804(1)	17.7939(9)	17.840(1)	9.7990(2)	15.8297(3)	8.392(1)
b/Å	14.255(4)	14.131(1)	14.3421(9)	14.251(1)	37.641(1)	10.8577(3)	12.611(2)
c/Å	12.199(3)	12.3169(8)	11.9338(5)	12.3267(6)	12.3724(3)	16.0071(5)	25.993(5)
β/°	129.34(1)	129.00(1)	129.008(2)	129.535(3)	93.016(1)	93.859(2)	
V/Å³	2394(1)	2408.1(3)	2366.6(2)	2417.0(2)	4557.2(2)	2745.0(1)	2750.9(8)
Space group	Cc (no. 9)	Cc (no. 9)	Cc (no. 9)	Cc (no. 9)	$P2_1/n$ (no. 14)	$P2_1/c$ (no. 14)	$P2_12_12_1$ (no. 19)
μ/mm⁻¹	0.221	0.220	0.225	0.304	0.224	0.309	0.201
Reflections measured	2184	7660	7591	6480	21036	17298	12891
Unique reflections	2184	2828	2800	2798	9122	6436	2922
Reflections used in refinement [$I > 2\sigma(I)$]	1887	1953	2327	2221	5546	3836	1410
R_{int}	0.000	0.092	0.077	0.043	0.062	0.058	0.192
R/R_w (for data $I > 2\sigma I$)	0.043/0.120	0.089/0.229	0.063/0.146	0.049/0.098	0.064/0.136	0.060/0.108	0.086/0.186

stability constant K for the complexation was calculated from NMR chemical shifts using the Benesi–Hildebrand least-square line-fitting procedure.[11]

Crystal structures

The X-ray crystallographic data for complex **7** were recorded with an Enraf-Nonius CAD4 diffractometer and for all other complexes with a Nonius Kappa CCD diffractometer. Graphite monochromatised Mo-Kα radiation [λ(Mo-Kα) = 0.710 73 Å] and a temperature of 173.0 ± 0.1 K were used in all cases. The CCD data were processed with Denzo-SMN v0.93.0[15] and all structures were solved by direct methods (SHELXS-97[16]) and refined on F^2 by full-matrix least-squares techniques (SHELXL-97[17]). All complexes crystallised in monoclinic space groups except for DB21C7 complex **10**, which crystallised in an orthorhombic space group. The hydrogen atoms were calculated to their idealised positions with isotropic temperature factors (1.2 times the carbon temperature factor) and refined as riding atoms. The carbon C18 in complex **10** is disordered between two sites with occupancies of 0.596 : 0.404. The sulfur S27 and carbon C31 of complex **16** are disordered with site occupation factors of 0.561 and 0.439. See Table 3 for crystallographic data for compounds **7–10** and **14–16**.

Suitable single crystals for X-ray crystallography were obtained by slow evaporation of acetonitrile or using vapour diffusion of acetonitrile into toluene.

CCDC reference number 440/156. See http:/www.rsc.org/suppdata/nj/2000/a907608e for crystallographic files in. cif format.

FAB and ESI mass spectra

FAB (fast atom bombardment) mass spectra were obtained on a Kratos MS 80 mass spectrometer with a DART data system. The atom gun was operated at 8 keV and argon was employed as the bombarding gas. The stainless steel FAB probe was coated with a thin layer of 3-nitrobenzyl alcohol matrix solution (NBA, Aldrich-Chemie) and samples of equimolar quantities of host and guest compounds were deposited on the probe tip for recording the mass spectra. ESI (electrospray ionisation) mass spectra were obtained on a LCT (Micromass Ltd) time of flight mass spectrometer with OpenLynx3 Data system. The diluted sample mixture, host and guest compounds in acetonitrile solution, was directed by a Harvard 5311 syringe pump into the ZSPRAY electronspray source at a flow rate of 10 μl min⁻¹. The vaporiser temperature was 120 °C and N_2 was used as nebuliser (80 l h⁻¹) and desolvation (400 l h⁻¹) gas. The electrospray capillary was at 3.5 keV, the sample cone at 20 V (minimal fragmentation conditions) and the instrument resolution was 5000.

References

1 E. Weber and F. Vögtle, in *Comprehensive Supramolecular Chemistry*, ed. J. Atwood, J. Davies, D. MacNicol and F. Vögtle, Elsevier, Oxford, 1st edn., 1996, vol. 2, pp. 1–28.
2 (a) D. A. Dougherty, *Science*, 1996, **271**, 163; (b) J. C. Ma and D. A. Dougherty, *Chem. Rev.*, 1997, **97**, 1303.
3 (a) D. B. Amabilino, F. M. Raymo and J. F. Stoddart, in *Comprehensive Supramolecular Chemistry*, ed. J. Atwood, J. Davies, D. MacNicol and F. Vögtle, Elsevier, Oxford, 1st edn., 1996, vol. 9, pp. 86–127; (b) M. Lämsä, T. Suorsa, J. Pursiainen, J. Huuskonen and K. Rissanen, *Chem. Commun.*, 1996, 1443; (c) M. Lämsä, J. Huuskonen, K. Rissanen and J. Pursiainen, *Chem. Eur. J.*, 1998, **4**, 84; (d) M. Lämsä, J. Pursiainen, K. Rissanen and J. Huuskonen, *Acta Chem. Scand.*, 1998, **52**, 563.
4 T. B. Stolwijk, E. J. R. Sudhölter, D. N. Reinhoudt, J. van Eerden and S. Harkema, *J. Am. Chem. Soc.*, 1989, **54**, 1000.
5 J.-M. Lehn, P. Vierling and R. C. Hayward, *J. Chem. Soc., Chem. Commun.*, 1979, 296.
6 C. D. Gutsche and K. A. See, *J. Org. Chem.*, 1992, **57**, 4527.
7 J. Rebek, Jr., B. Askew, M. Killoran, D. Nemeth and F.-T. Lin, *J. Am. Chem. Soc.*, 1987, **109**, 2426.
8 S. Kiviniemi, A. Sillanpää, M. Nissinen, K. Rissanen, M. T. Lämsä and J. Pursiainen, *Chem. Commun.*, 1999, 897.
9 K. A. Connors, in *Binding Constants*, John Wiley & Sons, New York, 1987, pp. 189–200.
10 Y. Takahashi, S. Sankararaman and J. K. Kochi, *J. Am. Chem. Soc.*, 1989, **111**, 2954.
11 H. A. Benesi and J. H. Hildebrand, *J. Am. Chem. Soc.*, 1949, **71**, 2703.
12 L. J. Farrugia, *J. Appl. Crystallogr.*, 1997, **30**, 565.
13 D. D. Perrin, W. L. F. Amarego and D. R. Perrin, *Purification of Laboratory Chemicals*, 3rd edn., Pergamon, Oxford, 1998.
14 D. H. Bonsor, B. Borah, R. L. Dean and J. L. Wood, *Can. J. Chem.*, 1976, **54**, 2458.
15 Z. Otwinowski and W. Minor, *Methods in Enzymology, Macromolecular Crystallography, Part A*, ed. C. W. Carter, Jr. and R. M. Sweet, Academic Press, New York, 1997, pp. 307–326.
16 G. M. Sheldrick, SHELXS-97, A Program for Automatic Solution of Crystal Structures, University of Göttingen, Germany, 1997.
17 G. M. Sheldrick, SHELXL-97, A Program for Crystal Structure Refinement, University of Göttingen, Germany, 1997.

Paper a907608e